PREDICTING THE ENERGY DISSIPATION RATE IN A MECHANICALLY STIRRED TANK

Graeme LANE[1*]

[1] CSIRO Mineral Resources, Clayton, Victoria 3169, AUSTRALIA

*Corresponding author, E-mail address: Graeme.Lane@csiro.au

ABSTRACT

The fluid kinetic energy dissipation rate in a mechanically stirred tank is an important parameter in relation to many process applications. For example, the dissipation rate controls the rates of break-up or coalescence of bubbles or droplets in various multiphase processes. While the average dissipation rate may be estimated from the power input per unit volume, the details of the spatial distribution of the energy dissipation rate are also very important for many processes. However, energy dissipation rates are difficult to quantify, and in simulations of stirred tanks using computational fluid dynamics (CFD), dissipation rates have generally been poorly predicted.

CFD modelling was carried out to investigate the energy dissipation in a tank stirred by a Lightnin A310 impeller, following a configuration for which experimental measurements have been published (see Bugay et al., 2002). Initial modelling results were compared for the k-ε and Shear Stress Transport (SST) turbulence models, and it was found that the SST model was more accurate in terms of overall flow characteristics; however, dissipation rates were substantially underpredicted.

Further development was therefore undertaken, which initially focussed on improving the mesh design and increasing the mesh density. Additional turbulence models were also assessed. Through this work, improved predictions of the dissipation rate were obtained, with integration of the dissipation rate over the tank volume yielding 90% of the expected power input. It was found that ~30% of the energy was dissipated in a small 'control volume' around the impeller, compared to an estimate of 40% from measurements. Further modelling was carried out using the Detached Eddy Simulation method. With this approach, the integrated dissipation rate was only 70% of the power input, however the dissipation within the impeller 'control volume' was again 30% of the predicted total dissipation.

NOMENCLATURE

D impeller diameter [m]
k turbulent kinetic energy per unit mass [$m^2 s^{-2}$]
N impeller rotation speed [s^{-1}]
P power [W]
S shear strain rate [s^{-1}]
V volume [m^3]
ε rate of dissipation of turbulent kinetic energy per unit mass [W/kg]
μ dynamic viscosity [Pa s]
μ_T eddy viscosity [Pa s]
ρ density [kg m^{-3}]
DES   detached eddy simulation
LES   large eddy simulation
EARSM Explicit Algebraic Reynolds Stress Model
SST   Shear Stress Transport model
SST-CC Shear Stress Transport with curvature correction
SST-RM Shear Stress Transport with reattachment modification
SST-RM-CC Shear Stress Transport with reattachment modification and curvature correction

INTRODUCTION

The rate of dissipation of fluid kinetic energy in mechanically stirred tanks is an important parameter for characterising the process behaviour in many applications. It is a controlling factor for phenomena including mass transfer and micromixing. Furthermore, the energy dissipation rate determines the magnitude of the shear forces, which are important in multiphase processes, determining the conditions for break-up of bubbles or droplets, or the collision rates of particles leading to coalescence or agglomeration. In stirred tank bioreactors, cell cultures or enzymes may experience shear damage due to excessive levels of energy dissipation.

Stirred tanks are normally operated under turbulent conditions, in which case most of the energy input to the system is transferred into the fluctuating fluid motions as turbulent kinetic energy, which is transferred down an eddy cascade from large to small scales and then dissipated by viscosity. The dissipation of turbulent kinetic energy is the main contribution to the total dissipation rate, and is the form of energy dissipation considered in most studies, although there may be a small additional contribution due to direct dissipation by mean velocity gradients (George, 2013). The integration of the kinetic energy dissipation rate over the whole fluid volume is equal to the power input, and thus the power per unit volume represents an average dissipation rate, which has been used in various design correlations, such as correlations for droplet size or interphase mass transfer rate (Paul et al., 2004). Constant power per unit volume is often used as a scale-up rule. However, the details of the spatial distribution of the dissipation rate are also very important. Local values of dissipation in stirred tanks are known to vary over at least three orders of magnitude (Zhou et al., 1996), and in many cases the distribution of local values of energy dissipation controls the process behaviour. For example, droplets and bubbles may only break up in regions with a dissipation rate exceeding a threshold value, and the maximum shear rate rather than the mean may determine various process outcomes (Paul et al., 2004). Despite its importance, energy dissipation rates and their distribution in stirred tanks are generally not well known, since this quantity has proven extremely difficult to determine to a satisfactory level of accuracy, either from laboratory measurements (Kilander et al., 2005) or by CFD modelling (Yeoh et al., 2004).

A number of experimental studies have investigated the local energy dissipation rate in stirred tanks. This is a difficult task as it has not been feasible to make direct measurements, due to extremely high spatial resolution requirements. However, studies have been carried out by applying various approximate methods. Zhou and Kresta (1996) assessed the turbulent kinetic energy dissipation rate using an equation derived from dimensional analysis, for a number of different impellers including a Rushton turbine, a PBT and an A310. Kilander et al. (2005) compared different methods of estimation including analysis using dimensional arguments and the Large Eddy PIV approach. Bugay et al. (2002) applied a PIV technique to measure the turbulent kinetic energy and Reynolds stresses in the discharge of a Lightnin A310 impeller, and determined the rate of turbulent kinetic energy dissipation from a balance equation for the turbulent kinetic energy taking production and advection terms into account.

CFD modelling methods have been applied for many years for investigating the fluid flow in mechanically stirred tanks. In the majority of published studies, validation of the CFD model has usually been carried out with respect to the velocity field only, or sometimes including the turbulent kinetic energy, but the energy dissipation rate has rarely been considered, despite its importance as outlined above. Where considered, predictions of turbulent kinetic energy and its dissipation rate have usually been found to be quite poor (Yeoh et al., 2004; Gimbun et al., 2012). This is known to be the case even where there are no detailed data to compare local values, since integration of the predicted turbulent energy dissipation rate over the complete tank volume ought to yield a value close to the measured power input, but this has seldom been the case.

One study which considered the prediction of energy dissipation rates was reported by Murthy et al. (2008), who investigated CFD modelling with several impeller types including a disc turbine, pitched bladed turbines and a hydrofoil. They found that the power input was predicted adequately from the torque on the impeller, whereas integration of the energy dissipation rates obtained with either k–ε or a Reynolds stress transport model generally underpredicted the measured power. Singh et al. (2011) compared several different turbulence models for modelling the flow produced by a Rushton turbine, including k–ε, Shear Stress Transport (SST), the SSG Reynolds stress model, and SAS-SST. Overall, they found that the SST model with curvature correction was the best choice, but all turbulence models underpredicted the turbulent energy dissipation rate.

Limitations to the accuracy of RANS simulations may lie in the assumptions of the various turbulence models, e.g. an assumption of isotropy and the approximation of the various terms in the transport equations for turbulence quantities. This has led to interest in modelling of stirred tanks using other more detailed approaches, such as large eddy simulation (LES) (e.g. Hartmann et al., 2004; Murthy et al., 2008) or detached eddy simulation (DES) (e.g. Gimbun et al., 2012), although the energy dissipation predictions according to such methods have not often been evaluated. However, Yeoh et al. (2004) applied LES to a tank with a Rushton turbine and found that integration of the energy dissipation rate over the tank volume gave much closer agreement to the power input compared to RANS simulations. Murthy et al. (2008) also found closer

agreement with the power input using LES compared to RANS predictions.

In this study, CFD modelling methods have been applied to determine the distribution and magnitude of the energy dissipation rate in a tank stirred by a Lightnin A310 hydrofoil impeller. The aim of the investigation was to improve the predictions of the dissipation rate as evaluated by comparison with experimental data. The study has considered aspects of the modelling approach including the design of the finite volume mesh and the choice of turbulence model, and RANS simulations have also been compared with the Detached Eddy Simulation approach.

METHOD

This study has investigated a baffled tank stirred by a Lightnin A310 impeller, following the configuration used in an experimental study as reported by Bugay et al. (2002), who published detailed measurements of velocities and turbulent kinetic energy for various locations in the tank, and also estimated the turbulent energy dissipation rate in the impeller discharge flow. The cylindrical tank has an overall internal diameter of 0.45 m and the liquid depth is equal to the diameter. The tank is fitted with four baffles with a width equal to one tenth of the tank diameter and is stirred by a 0.15 m diameter Lightnin A310 impeller, which was located with a clearance of 0.15 m to the tank bottom.

The impeller speed in the experimental study was 200 rpm, giving an impeller Reynolds number of 75,000. However, for investigating predictions of the energy dissipation rate, the impeller speed was reduced to 80 rpm in the simulations (impeller Reynolds number of 30,000). This was done with a view to reducing the very high computational demands of the detached eddy simulation which was included in the study, where the time step in DES needs to be made smaller as Reynolds number increases. It was considered that comparison to the experimental study was still valid since the flow regime remains fully turbulent, and energy dissipation rates are expected to remain the same when expressed on a dimensionless basis (i.e. when scaled by the cube of the impeller speed).

The conservation equations for mass and momentum were solved using the ANSYS CFX software (Version 15) in conjunction with a turbulence model. Several turbulence models were tested, including k–ε, the SST model (including several modifications), and the Explicit Algebraic Reynolds Stress Model (EARSM). A further simulation was carried out using DES. For these simulations, a finite volume mesh was generated which included details of the baffles and the impeller. Care was taken to resolve the full three-dimensional shape of the A310 impeller, including the curved leading edge. The grid resolution was highest in the vicinity of the impeller blades since velocity gradients are very high in these regions. Inflation layers were used on the impeller blades and at all tank walls for accurate prediction of wall shear stresses. The A310 impeller is illustrated in Figure 1, where a typical mesh design is illustrated on an intersecting vertical plane.

To account for impeller rotation, two approaches were adopted. In the first approach, the Multiple Frames of Reference (MFR) method was used, where the section of the mesh surrounding the impeller remains in a single fixed position, but is in a rotating frame of reference. The second approach used the Sliding Mesh method, where the mesh around the impeller is rotated in small angular

2

increments and the flow is recalculated at each time step of a transient simulation. The second approach is more accurate, but it was found that MFR was adequate in the RANS simulations for comparing energy dissipation values, since predicted values were almost the same as with the Sliding Mesh method.

Convergence for each simulation was based on the criteria that the scaled residuals of all conservation equations fell below a factor of 10^{-4}, and also a steady mean flow pattern was obtained which did not change significantly with further iterations or time steps.
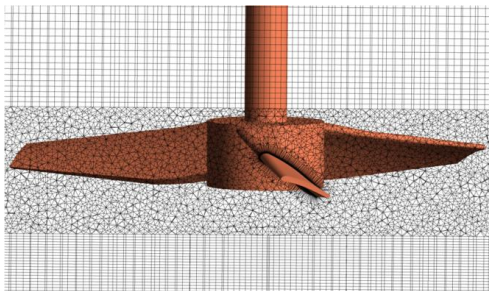

Figure 1: A310 impeller as constructed for CFD modelling, illustrating mesh construction around impeller as in initial stage with full tank model.

RESULTS

As a first step, simulations were carried out based on the full tank geometry to assess the overall accuracy of the modelling method. Two turbulence models were compared at this stage, being k–ε and SST. The k–ε model has been frequently used in the past for stirred tank simulations whereas, more recently, the SST model has been recommended as being more accurate (Singh et al., 2011). The SST model is claimed to have several advantages in dealing with wall-bounded flows. It provides more reliable predictions of flow separation. Also, wall boundary conditions for the turbulent parameters are formulated better, and an 'automatic' treatment is incorporated for modelling boundary layers, which adjusts smoothly from wall function calculations to direct integration as the mesh is refined.

Simulations of the full tank were based on a mesh containing a total of 3.19 million nodes, with the near-wall mesh refined so as to obtain wall y^+ values of less than 2 on the impeller and less than 70 on the walls. The Sliding Mesh method was used.

The predicted fluid flow pattern is illustrated by Figure 2, showing the mean velocity field in a vertical plane using the SST model, while Figure 3 shows the corresponding distribution of the turbulent kinetic energy dissipation rate. Detailed comparisons with measurements of Bugay et al. (2002) were carried out for the axial velocity component, turbulent energy and turbulent energy dissipation rate on plane just below the impeller. SST showed better agreement with the velocity profile below the impeller, and also predicted flow separation on upper side wall in agreement with the measurements, which k–ε failed to predict. The peak values of turbulent kinetic energy and turbulent energy dissipation rate were closer to the experimental values with k–ε, but SST predicts the shape of the curves better (see Figure 4). This suggests that k–ε does not provide a good prediction of the flow structure around the impeller blades.

The total energy dissipation rate in the tank was calculated from the simulations taking into account both the turbulent energy dissipation and the viscous dissipation due to the resolved flow field. The volume integrated energy dissipation rate is then calculated according to:

$$P_{CFD} = \int (\rho\varepsilon + \mu S^2)\ dV \qquad (1)$$

where ρ is the fluid density, ε is the turbulent kinetic energy dissipation rate, μ is the molecular viscosity and S is the mean flow shear strain rate. The predicted total dissipation may be compared with the expected power input based on a reported impeller power number of 0.3 (Bugay et al., 2002). Also, Bugay et al. (2002) made an estimate that the dissipation within a small 'control volume' surrounding the impeller, being a cylindrical volume with radius equal to that of the impeller and extending from 0.145 m to 0.18 m from the bottom, represents 40% of the total power input. For comparison, the predicted dissipation according to the CFD simulations is also reported for this region.

The predicted integrated dissipation rates from all simulations are summarised in Table 1. For the full tank simulations, the total dissipation represented 80% of the expected power input when using k–ε, whereas with the SST model, the integrated dissipation gave 68% of the expected power. With k–ε, 28% of the predicted dissipation was within the impeller control volume, compared to only 16% for SST. Thus, in terms of integrated dissipation values, the k–ε model seems more satisfactory. However, predictions with k–ε in terms of the flow pattern and the spatial distribution of turbulence were not satisfactory, and overall, SST seems to be a preferable choice of turbulence model.
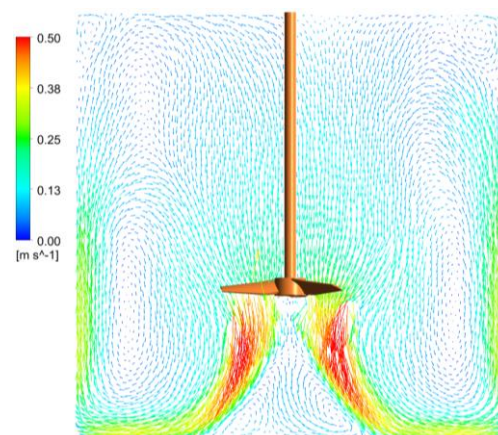

Figure 2: Time-averaged fluid velocity in a vertical plane: full tank geometry with SST turbulence model.

Further modelling was carried out with aim of improving predictions of the energy dissipation rate, initially using the SST model. The low energy dissipation rates predicted for the impeller region suggested that better modelling was needed in this region. It was found that tip vortices are generated on the impeller blades creating regions of intense circulation, which suggested that the velocity gradients near the impeller blades might be underestimated due to insufficient mesh resolution, in which case there would be insufficient turbulence production by the CFD model. Various other studies (e.g. Karcz et al., 2012) have found that increasing the mesh resolution leads to increased values of turbulent kinetic energy and its dissipation rate. Therefore, further simulations were carried out with increased mesh

resolution. In order to maximise the resolution while managing the computational cost, these simulations were based on modelling of just one impeller blade only. This approach is somewhat problematic since no simple plane of symmetry is available to reduce the problem size. However, it is possible to define regions of different circumferential extent in ANSYS CFX, by specifying a pitch change at the interface. This was done so as to model just one impeller blade in a 120° section, coupled to a 180° section of the tank containing two baffles. Periodic boundaries were assumed in the circumferential direction, while the MFR approach was used for impeller rotation in conjunction with the 'stage' method, where velocities and pressure are averaged across the interface.
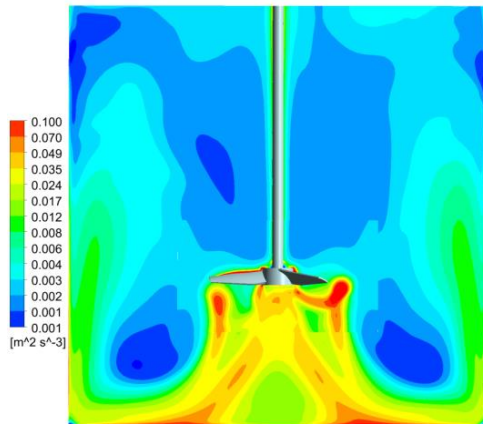

Figure 3: Time-averaged turbulent kinetic energy dissipation rate in a vertical plane: full tank geometry with SST turbulence model (note logarithmic scale).
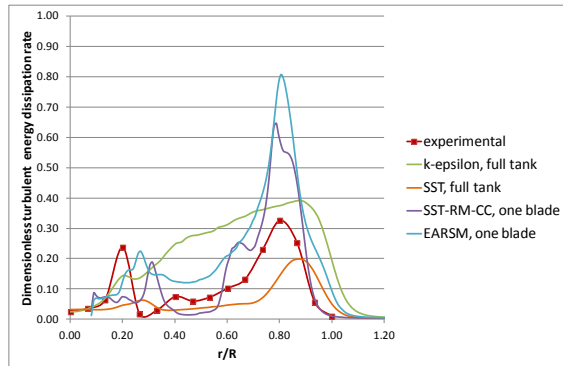

Figure 4. Radial profile of dimensionless turbulent energy dissipation rate (ε/N^3D^2) on a plane just below the impeller ($z = 0.145$ m): comparison of estimated values according to Bugay et al. (2002) with predictions based on full tank geometry using k–ε or SST models with mesh of 3.17 M nodes, and with single impeller/half tank geometry using SST RM CC or EARSM with 10.4 M nodes.

Simulations were carried out in which the mesh was progressively refined, but in a non-uniform way, where the extra nodes were mainly added in regions of high velocity gradients, mostly in the vicinity of the impeller blade and with highest density in an annular region covering the path of the tip vortex. Comparison of the integrated dissipation rates with the expected input power (Table 1) showed a progressive increase in predicted values when the mesh size increased from 3.4 million to 10.4 million nodes, but with a further increase to 21.5 million nodes, there was no further increase in the predicted dissipation. Thus, from a

point of view of obtaining mesh-independent results, the mesh with a total of 10.4 million nodes seems adequate, at least for the SST model. With this mesh, most of the nodes are concentrated near the impeller, with 8.4 million nodes in the impeller subdomain.

Based on the mesh of 10.4 million nodes, further simulations were carried out to investigate the effect of the turbulence model. At this mesh resolution, the k–ε and SST models yielded similar values for the integrated energy dissipation rate over the whole tank and in the impeller control volume, but the results with SST remained much more satisfactory in terms of the predicted flow structure near the impeller and in the bulk of the tank. Further testing was carried out for two variations of the SST model. Firstly, the curvature correction (SST-CC) was included, in which case the production term in the turbulent kinetic energy equation is modified to account for streamline curvature. Simulations were also run including the Reattachment Modification (SST-RM), which attempts to address the issue of underprediction of turbulence production in regions of massive flow separation (CFX Solver Manual, 2015). A further variation was tested incorporating both of these modifications (SST-RM-CC). Simulations were also carried out using the Explicit Algebraic Reynolds Stress Model (EARSM). This is an extension to the two equation BSL k–ω model, which calculates the anisotropy tensor by solving an implicit matrix equation (CFX Solver Manual, 2015).

Table 1 compares the volume integrated energy dissipation rates for the various turbulence modelling options. With SST, the total dissipation rate is equal to 84% of the expected power using the higher mesh density. Further increases are obtained with other turbulence models. With the SST-RM-CC and EASRM models, the integrated energy dissipation reaches 89–91% of the expected power input, and the dissipation in the impeller control volume is about 29%, which approaches more closely to the estimate of 40% according to Bugay et al. (2002) compared to the earlier simulations with lower mesh density. It can be noted that the contributions due to the resolved, mean flow velocity gradients are significant in these simulations, especially in the impeller control volume, where resolved flow dissipation is about 30% of the total. The contributions from the resolved flow field are mainly due to viscous dissipation in the boundary layers.

In Figure 4, profiles for the turbulent kinetic energy dissipation rate below the impeller are shown again for the 10.4 million node grid, using SST-RM-CC or EARSM models. The values are now in better agreement with the estimates of Bugay et al. (2002), except that the main peak value is now considerably higher according to CFD predictions. This larger peak value perhaps reflects a higher mesh resolution in the CFD compared to the resolution of the measured velocity field upon which the experimental estimates were based.

The high resolution simulations provide detailed information regarding the flow around the impeller, as illustrated by Figures 5–7. Velocity vector plots (Figures 5– 6) indicate a large region with flow separation from the upper blade surface, and formation of the tip vortex. The tip vortex is visualised in Figure 7 by means of a vorticity isosurface plot. The peak value of turbulent dissipation rate was also determined from the simulations, and this was found to occur near the impeller blade tip with a value about 5000 times the average over the whole tank.

Further investigation was carried out using a Detached Eddy Simulation (DES) method. Like LES, this approach aims to avoid various limitations of RANS turbulence models by resolving the large, geometry-dependent turbulent eddies while modelling only the small eddies of universal character. LES has been carried out in several studies for stirred tanks, but this approach has been criticised (Menter, 2012) as being inappropriate for wall-bounded flows, since the turbulence in the boundary layers is not properly resolved unless prohibitively high mesh resolution are used. For improved modelling, various blended schemes have been proposed, where LES is applied in regions away from walls while still using RANS models close to walls. One such method is DES, which was tested here using the version as implemented in ANSYS CFX, in which the SST model applies to the near-wall regions, while away from walls a switching criterion based on the grid size is applied to modify the production term in the k equation and reduce eddy viscosity, resulting in LES behaviour (CFX Solver Manual, 2015).

To meet the requirements of DES, some changes were made to the mesh design. Again, only one impeller blade was modelled, but to model turbulent structures it was necessary to establish a 1:1 correspondence between the interface areas of the impeller and bulk subdomains. Therefore, a 1/3 tank section was modelled, containing just one baffle. The flow pattern changes somewhat due to the reduced level of baffling, but the flow pattern near the impeller and the distribution of dissipation rates remained similar. The mesh near the impeller was further refined to meet the requirement that, outside of the boundary layers, the mesh spacing as measured by maximum edge length is everywhere less than the turbulent length scale as calculated from a previous RANS solution (CFX Solver Manual, 2015). This requirement led to a mesh consisting of about 13.1 million nodes. A transient simulation was run using the Sliding Mesh option for impeller rotation, and the time step was specified to give a RMS Courant number of 0.8. The simulation was run for a sufficient number of time steps so as to bring the simulation into equilibrium. Figure 8 shows a plot of vorticity near the impeller blade, illustrating the prediction of turbulent structures by this method.

Dissipation rates obtained from DES were evaluated separately for the RANS and LES zones. In the LES region, the total rate of energy dissipation was evaluated based on the dissipation at both resolved and subgrid scales (Hartmann et al., 2004; Yeoh et al., 2004), which was integrated to estimate the power input according to:

$$P_{CFD} = \int (\mu + \mu_T) S^2 \, dV \qquad (2)$$

where μ is the molecular viscosity, μ_T is the eddy viscosity and S is the shear strain rate of the resolved flow field. The total integrated energy dissipation added up to only 70% of expected power input. It is likely that an even higher mesh resolution is required here for predicting dissipation rates, which is indicated by the large portion of the energy dissipation which remains unresolved and is represented by the subgrid eddy viscosity. In any case, the DES is consistent with the RANS results in terms of the distribution of the energy dissipation rate. The energy dissipation within the control volume around the impeller was again about 30% of the total.

CONCLUSION

This study indicates that adequate prediction of energy dissipation rates can be obtained from CFD modelling, but this is strongly dependent on the use of a sufficiently high resolution finite volume mesh of an appropriate design, in combination with the choice of an appropriate turbulence model. For simulations of a tank stirred by a Lightnin A310 and using a reduced geometry containing one impeller blade only, it was found that a grid of about 10.4 million nodes total was required when solving the RANS equations, with most of the mesh nodes being concentrated near the impeller. Up to about 90% of the expected power input could then be obtained from integration of the mean and turbulent kinetic energy dissipation, with the best results being for either the SST model (including curvature correction and reattachment modification), or the EARSM. These models are also preferable, especially compared to k-ε, since the predicted flow structure is in better agreement with measurements.

A DES simulation was also carried out as an alternative to RANS turbulence modelling. Only 70% of power input was found here from integration of the dissipation rates, suggesting a need for higher mesh resolution; however, the DES results were consistent with those from RANS in terms of the distribution of energy dissipation, with the dissipation in the impeller 'control volume' being about 30% of the total with either method, compared to an estimate of 40% according to Bugay et al. (2002).
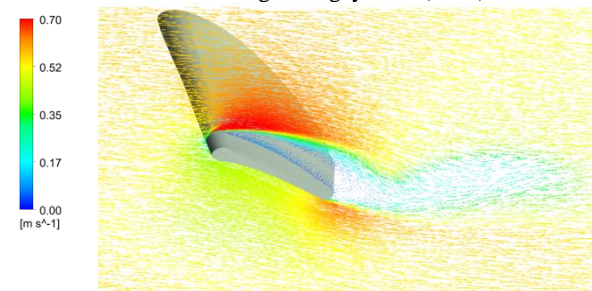

Figure 5: Projected velocity vectors relative to impeller motion in a vertical plane perpendicular to the impeller blade, showing flow separation (SST-RM-CC model with grid of 10.4 M nodes).
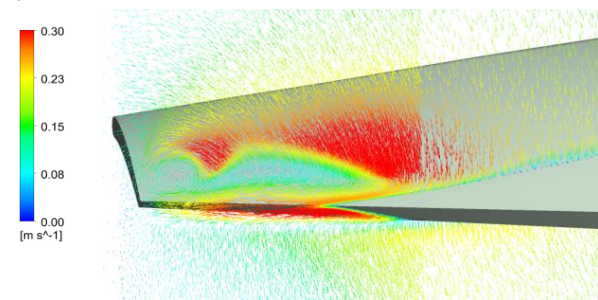

Figure 6: Projected velocity vectors relative to impeller motion in a vertical plane perpendicular to the tip vortex, showing flow separation and tip vortex formation (SST-RM-CC model with grid of 10.4 M nodes).

A further comment for the A310 is that a model of the full tank may be required in some circumstances to obtain the most realistic simulation of the flow pattern. In that case, a mesh of about 28 million nodes is indicated by this study for adequate prediction of the energy dissipation rates. A mesh of this size is likely to be impractical at present in many situations (e.g. more complex multiphase simulations), but it is suggested that a spatially-dependent correction factor might be applied to the dissipation rates in simulations with smaller mesh sizes, based on the values and distribution obtained in a simulation using a high resolution mesh.

Table 1: Summary of the predicted energy dissipation rates in each simulation, integrated over the tank volume and over the impeller 'control volume', with comparison to expected power input.

Configuration	No. of mesh nodes ($\times 10^6$)	Turbulence model	Total dissipation as % of expected power input	Dissipation in full tank as % of total predicted		Dissipation in impeller control vol. as % of total predicted		
				Turbulent/ sub-grid	Mean /resolved	Turbulent/ sub-grid	Mean /resolved	Total[1]
Full tank	3.17	k–ε	80	99.4	0.6	27.6	0.02	28.0
Full tank	3.17	SST	68	94.4	5.6	11.1	4.8	15.9
1 impeller blade, half tank	3.4	SST	73	88.7	11.3	13.9	5.7	19.6
1 impeller blade, half tank	3.4	SST-RM	77	90.0	10.0	15.7	5.4	21.1
1 impeller blade, half tank	10.4	k–ε	87	98.4	1.6	28.5	1.0	29.5
1 impeller blade, half tank	10.4	SST	84	86.6	13.4	20.3	8.5	28.8
1 impeller blade, half tank	10.4	SST-CC	77	83.0	17.0	20.4	10.5	30.9
1 impeller blade, half tank	10.4	SST RM	91	88.2	11.8	19.8	7.7	27.5
1 impeller blade, half tank	10.4	SST-RM-CC	89	86.6	13.4	20.8	8.6	29.4
1 impeller blade, half tank	10.4	EARSM	91	89.3	10.7	21.5	7.7	29.2
1 impeller blade, half tank	21.5	SST	81	86.8	13.2	18.9	8.6	27.5
1 impeller blade, 1/3 tank	13.1	DES	69	59.1	40.9	13.6	15.1	28.7

[1]For comparison, the dissipation in the impeller control volume was estimated to be 40% of the total dissipation according to the experimental study of Bugay et al. (2002).
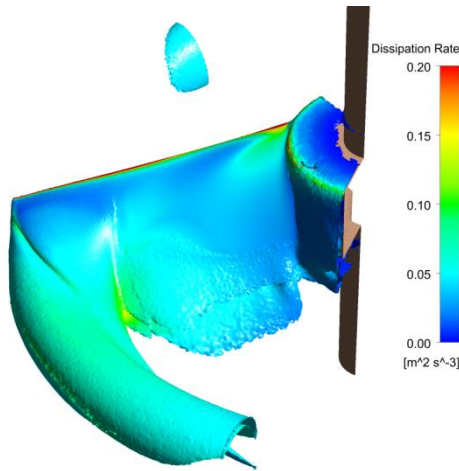

Figure 7: Isosurface of vorticity (= 40 s^{-1}) in vicinity of impeller blade coloured by energy dissipation rate, using EARSM turbulence model with mesh of 10.4 million nodes.
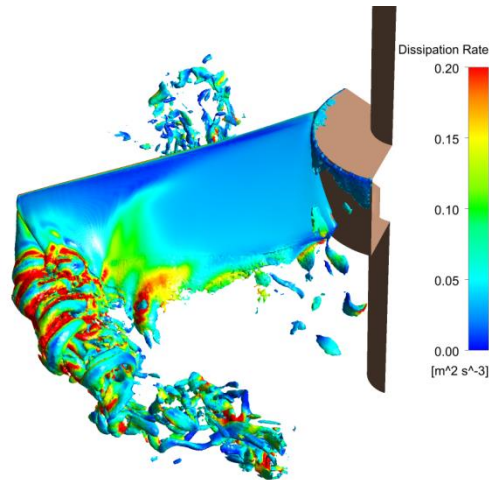

Figure 8: Isosurface of vorticity (= 200 s^{-1}) in vicinity of impeller blade coloured by energy dissipation rate, using Detached Eddy Simulation method with mesh of 13.1 million nodes .

REFERENCES

BUGAY, S., ESCUDIÉ, R., and LINÉ, A. (2002), 'Experimental analysis of hydrodynamics in axially agitated tank', *AIChE. J.*, **48** (3), 463–475.

CFX Solver Manual, ANSYS, Inc., 2015.

GEORGE, W.K. (2013), 'Lectures in Turbulence for the 21st Century', accessed online on 17/6/2015 at: www.turbulence-online.com/Publications/Lecture_Notes/ Turbulence_Lille/TB_16January2013.pdf

GIMBUN, J., RIELLY, C.D., NAGY, Z.K. and DERKSEN, J.J., (2012), 'Detached eddy simulation on the turbulent flow in a stirred tank', *AIChE J.*, **58** (10), 3224–3241.

HARTMANN, H., DERKSEN, J.J., MONTAVON, C., PEARSON, J. HAMILL, I.S. and VAN DEN AKKER, H.E.A. (2004), 'Assessment of large eddy and RANS stirred tank simulations by means of LDA', *Chem. Eng. Sci.*, **59**, 2419–2432.

KARCZ, J. and KACPERSKI, L. (2012), 'An effect of grid quality on the results of numerical simulations of the fluid flow field in an agitated vessel', *14th European Conference on Mixing,* Warsaw, 10-13 September 2012.

KILANDER, J. and RASMUSON, A. (2005), 'Energy dissipation and macro instabilities in a stirred square tank investigated using an LE PIV approach and LDA measurements', *Chem. Eng. Sci.*, **60**, 6844–6856.

MENTER, F.R. (2012), *Best Practice: Scale-Resolving Simulations in ANSYS CFD,* Version 1.0, ANSYS, Inc.

MURTHY, B.N. and JOSHI, J.B. (2008), 'Assessment of standard k–ε, RSM and LES turbulence models in a baffled stirred vessel agitated by various impeller designs', *Chem. Eng. Sci.,* **63** (5), 468–495.

SINGH, H., FLETCHER, D.F., and NIJDAM, J.J. (2011), 'An assessment of different turbulence models for predicting flow in a baffled tank stirred with a Rushton turbine', *Chem. Eng. Sci.,* **66**, 5976–5988.

PAUL, E.L. ATIEMO-OBENG, V.A., and KRESTA, S.M. (2004), *Handbook of Industrial Mixing: Science and Practice*, John Wiley and Sons, Inc.

YEOH, S.L., PAPADAKIS, G. and YIANNESKIS, M. (2004), 'Numerical simulation of turbulent flow characteristics in a stirred vessel using the LES and RANS approaches with the sliding/deforming mesh methodology', *Chem Eng. Res. Des.*, **82** (A7), 834–848.

ZHOU, G. and KRESTA, S. (1996), Impact of Tank Geometry on the Maximum Turbulence Dissipation Rate for Impellers, *AIChE J.*, **42** (9), 2476–2490.